A STATOR-CONTROLLED MAGNETIC BEARING

H. Ming Chen[1]

ABSTRACT

The magnetic bearing concept has a movable stator with no protruding poles. The radial magnet flux at the uniform air gap between the stator and rotor generated by using a permanent magnet or magnetizing coil, form an unstable bearing. To make it stable, the stator is mounted on mechanical springs and motion-controlled by feeding back the rotor displacement. The motion control actuator is likely a stationary magnetic bearing. Presented herein are a design methodology for the bearing concept and experimental results proving its feasibility. The bearing is best suited for supporting high speed rotors, such as those of energy or momentum storage flywheels, because it has minimal eddy-current loss and electronically maneuverable stiffness and damping.

INTRODUCTION

A conventional active magnetic bearing (AMB) has stationary electromagnetic poles around its rotor. The rotor surface material comes in and out of the magnetic flux of the protruding poles. The changing flux generate heat on rotor due to magnetic hysteresis and eddy current. The eddy current heat loss on high speed rotors even laminated can be a serious problem, because it is proportional to the square of rotor speed times number of poles, and difficult to dissipate in vacuum. It may result in high rotor temperatures causing stress or other thermal related problems. Using a homopolar AMB with extended pole edges in the circumferential direction may reduce the eddy current heat, but can not totally eliminate it. This has led to the use of continuous ring pole permanent magnetic (PM) bearings. Since the magnetic flux of the ring-shaped poles are not interrupted during rotation, the eddy current and hysteresis core losses can be kept to a minimum. As an example, two radial PM ring bearings have been designed for a flywheel energy storage power quality application (Chen and Walton, 1996). These bearings have stationary and rotating disks packed with several axially polarized PM rings. They are difficult to fabricate and have centrifugal stress concern in high speeds. Also, they have no damping; and their large axial negative stiffness require oversized active thrust magnetic bearings. To circumvent the problems, herein a bearing concept called stator-controlled magnetic bearing (SCMB) is presented (Chen, 1997). As shown in Figure 1, the stator consists of cylindrical sections of magnetic material and a PM ring axially polarized for generating magnetic flux.

[1]Mohawk Innovative Technology, Inc., 437 New Karner Road, Albany, NY 12205, USA.

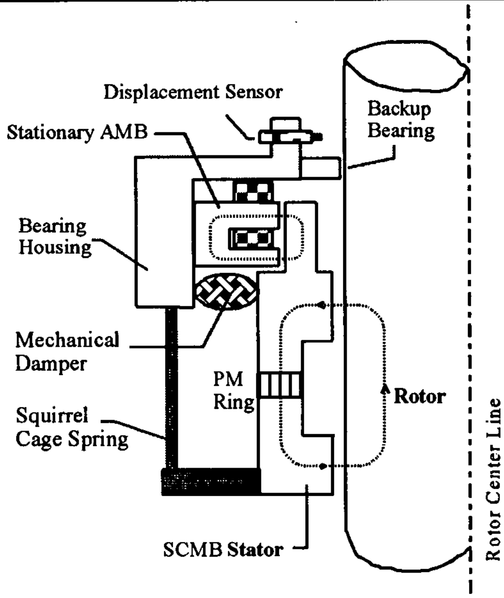

Figure 1 - A Stator-Controlled Magnetic Bearing

The rotor is simply a circular cylinder made of magnetic material with an outer diameter slightly smaller than the stator hole. The magnetic flux circulating through the annular air gaps between the stator and rotor create an unstable magnetic bearing with a negative stiffness. To make a stable bearing, the stator should be mounted on mechanical springs and its motion be controlled with feedback of the rotor motion (Oka and Higuchi, 1994). The latter are measured by using two displacement sensors. The actuator for controlling the stator motion is likely a stationary type of AMB.

A mathematical model of the bearing will be presented emphasizing on how to choose the bearing parameters for a desired performance. To demonstrate the concept feasibility, an experimental flywheel rotor and bearing device including a SCMB has been built and successfully tested.

MATHEMATICAL MODEL

There are two independent stator motion-control axes. The dynamics of each control axis can be represented by Figure 2. The equations of motions are:

$$M_s X_s'' = K_m(X_s - X_b) - F_s \tag{1}$$

$$M_b X_b'' = -K_m(X_s - X_b) - KX_b - CX_b' + F \tag{2}$$

M_s = rotor mass at bearing
M_b = stator mass
X_b = stator displacement
F_s = static load on rotor
F = stator control force
X_s = rotor displacement

', " = differentiate once, twice with respect to time
K_m = stiffness coefficient of magnetic field in air gaps
K = stiffness coefficient of stator mechanical support
C = damping coefficient of stator mechanical support

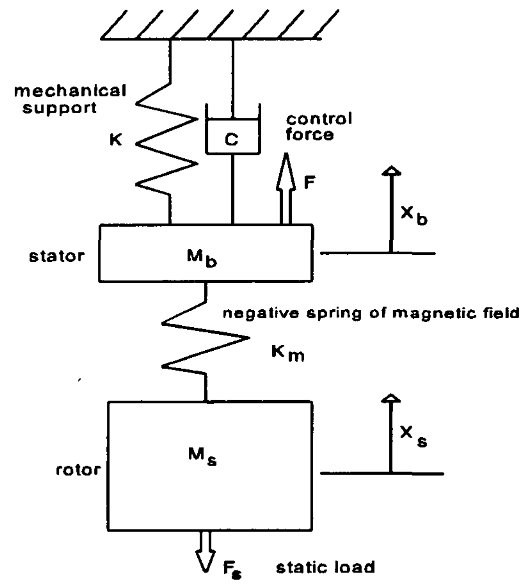

Figure 2 - Control Axis Representation

For the stator feedback control, the absolute rotor displacements are measured in two orthogonal directions. A PID (proportional, integral, derivative) control scheme is appropriate for the application and the stator control force is:

$$F = C_p X_s + C_d X_s' + C_i \int X_s dt \qquad (3)$$

where

C_p = proportional constant
C_i = integral constant
C_d = derivative constant
t = time

For evaluating stability, the static force F_s in equation (1) is ignored. Taking and combining Laplace transform of (1), (2) and (3), the following normalized system characteristic equation is obtained:

$$\mu S^5 + CS^4 + (K-\mu-1)S^3 + (C_d-C)S^2 + (C_p-K)S + C_i = 0 \qquad (4)$$

where S=Laplace variable and $\mu = M_b/M_s$. The parameters in (4) are normalized quantities as defined below:

$$S \Longrightarrow S/B_s$$
$$C \Longrightarrow C/\sqrt{K_m M_s}$$
$$C_d \Longrightarrow C_d/\sqrt{K_m M_s}$$
$$K \Longrightarrow K/K_m$$
$$C_p \Longrightarrow C_p/K_m$$
$$C_i \Longrightarrow C_i/K_m B_s$$

where the sign "==>" means "imply"and $B_s = \sqrt{K_m/M_s}$.

The above normalization is performed with respect to the magnetic stiffness (negative spring rate) K_m between the rotor and stator, and the rotor mass M_s which are the basic given quantities of the bearing system. The artificial parameter B_s provides a calibration of the system frequencies or how stiff the bearing is.

It is imperative to determine a set of values for μ, K, C, C_p, C_d and C_i, so that equation (4) has stable roots in the left half of S-plane. Out of the six parameters, only the mass ratio μ may be independently chosen. The rest five normalized parameters can be determined by using pole-placement method. A desirable set of five roots of the normalized equation (4) may include a pair or two of reasonably damped complex conjugate roots. This method will be demonstrated in the following test bearing design.

EXPERIMENT

To demonstrate the feasibility of the SCMB concept, a vertical rotor supported by a ball bearing and a SCMB as shown in Figure 3 has been designed, built and tested. The top deep-groove ball bearing served also as a thrust bearing taking the whole rotor weight. The rotor was driven at the top through a flexible coupling by a variable speed motor with a maximum speed of 10,000 rpm. The SCMB at bottom had the approximate rotor dimensions of 25 mm (1") in diameter and 25 mm (1") in length. The bending mode natural frequency was well above the maximum speed. The SCMB was expected to control predominantly the rigid-body mode with a "swinging pendulum" mode shape pivoted at the ball bearing.

The rotor mass (M_s) seen by the SCMB and the stator mass (M_b) were estimated to be 1.02 Kg (2.25 lb) and 0.22 Kg (0.48 lb), respectively. Therefore, the mass ratio μ (M_b/M_s) was 0.21. Note that because of relative low speed, the flux generating PM ring was mounted on the rotor for easy fabrication and stator weight reduction. The magnetic flux between the rotor and stator was estimated to be about 5000 gauss and confirmed with a flux measurement. The corresponding negative stiffness (K_m) was calculated (Knospe and Stephens, 1996) as approximately 87.5×10^3 N/m (500 lb/in). The reference frequency was:

$$B_s = \sqrt{K_m/M_s} = 293 \text{ radian/sec} = 46.6 \text{ Hz}$$

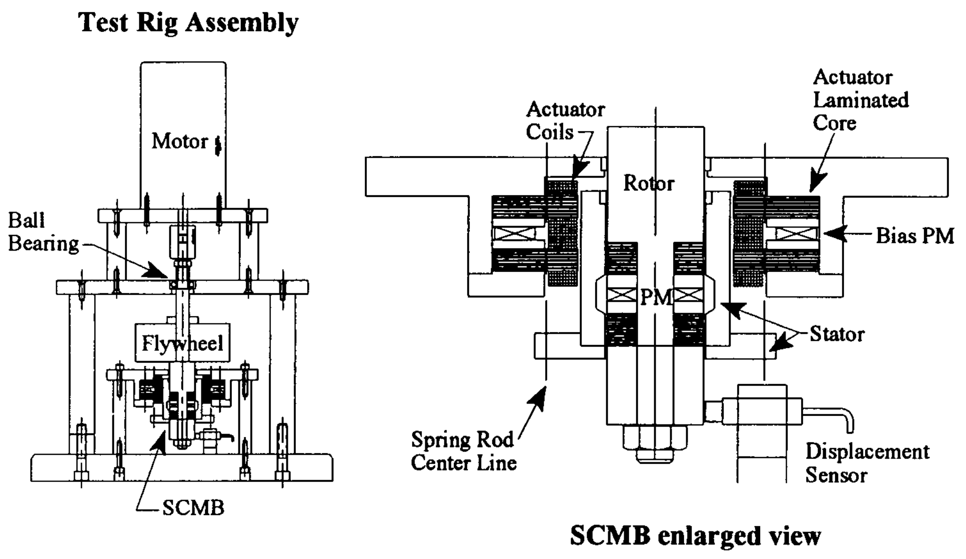

Figure 3 - SCMB Test Rig

POLE PLACEMENT

Let's consider the following five "desirable" roots:

$$= -0.5 \pm 0.5j\ ;\quad -0.5 \pm 0.5j\ ;\quad -0.25$$

This implied that the controlled system natural frequency would be at 23.3 Hz (= 0.5 B_s) or about 1400 rpm. The system characteristic equation can be re-created as:

$$[(S+0.5+0.5j)(S+0.5-0.5j)]^2(S+0.25) = 0 \qquad (5)$$

Comparing (5) to (4) with μ equal to 0.21, the following five normalized system parameters were obtained:

$$C = 0.48\ ;\ K = 1.75\ ;\ C_d = 0.80\ ;\ C_p = 1.86\ ;\ C_i = 0.013$$

We have thus defined the mechanical stiffness and damping for supporting the stator, and the PID gains for controlling the stator.

TRANSIENT SIMULATION

To test the performance of the system with the above parameters, a transient simulation of the rotor lifting off a backup bearing has been performed. The transient results as presented in Figure 4 and Figure 5 show the rotor and stator displacements and the associated forces along a control axis. The force exerted on rotor by stator is defined as $F_m = K_m(X_s\text{-}X_b)$, and the force applied by the actuator to the stator, i.e. the control force, is denoted by F.

One may use the transient analysis result to explain how the SCMB works. For example in Figure 4, before lift-off the rotor leaned on a backup bearing 0.08 mm (0.003 inch) away from the center, while the stator leaned on an opposite side stop, 0.20 mm (0.008 inch) away. The stator then moved over toward the shaft side to create lifting force when the control began. The amount of over-shooting rotor displacement is related to the real parts of the chosen complex conjugate roots. The maximum amplitude of the actuator control force F as shown in Figure 5, is dictated by the rotor backup bearing clearance. In this case, the backup bearing clearance was 0.08 mm and the maximum actuator force was 11.5 N (2.5 lb).

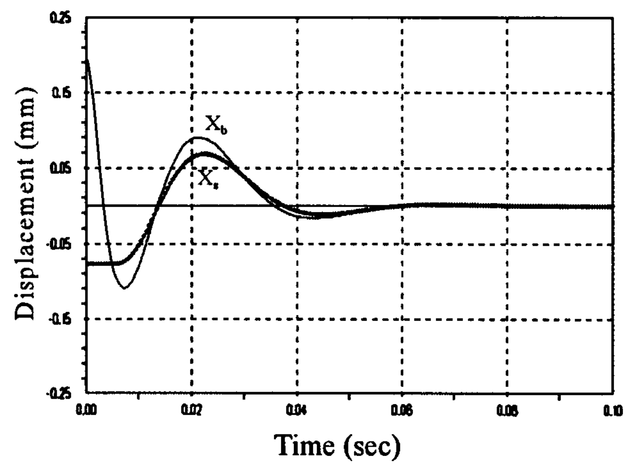

Figure 4 - Stator and Rotor Transient Displacement

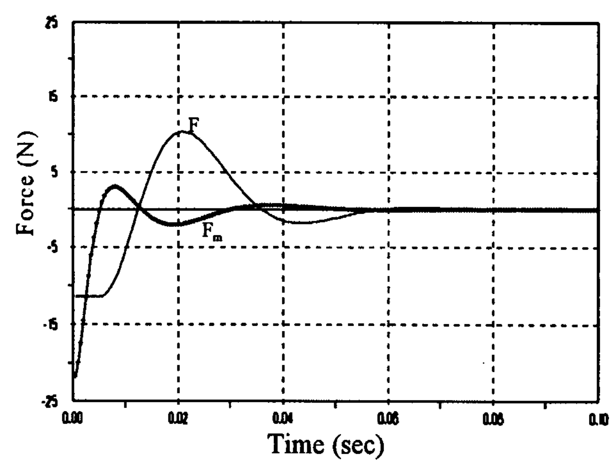

Figure 5 - Actuator and Rotor Transient Forces

ACTUATOR DESIGN

A homopolar electromagnetic device using permanent magnets for flux bias as shown in Figure 6 was the actuator. A part of the stator cylinder inside the device (Figure 3) served as the armature. The concentric gap was 0.76 mm (0.030 inch). The bias flux was about 4000 gauss corresponding to a negative spring rate of 73.5×10^3 N/m (420 lb/in). Using 50 coil turns per pole, The actuator could generate about ±36 N (±8 lb) of force using ±4 ampere of current. The actuator was designed to apply a force to the stator for any given input command with no significant time delay. The force which should be proportional to the flux difference of the opposite quadrants, was regulated using four Hall-effect probes, one for each quadrant as shown in Figure 7.

The stator was supported by four flexible steel rods working like guided cantilever beams. Therefore, the stator position was always in parallel with the rotor. The total spring rate of the rods minus the actuator negative spring rate and plus the damper stiffness contribution should be equal to 1.75 K_m or 153×10^3 N/m (875 lb/in), recalling that the required normalized mechanical stiffness was 1.75. Presented in picture of Figure 8 are the flexible rods, the Hall-effect probes and their pre-amplifiers.

The required mechanical damping should be:

$$C = 0.48 \sqrt{K_m M_s} = 144 \text{ N-sec/m} \quad (0.82 \text{ lb-sec/in})$$

It was originally implemented with a shear damper using an elastomer material. The shear damper material required a certain amount of compression which was difficult to adjust inside the actuator. During the tests, the damper was replaced with a more precise and controllable electronic scheme employing stator velocity feedback.

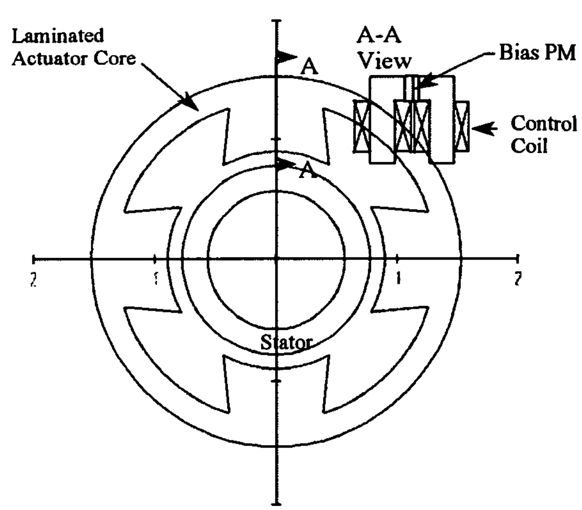

Figure 6 - Actuator Homopolar Core

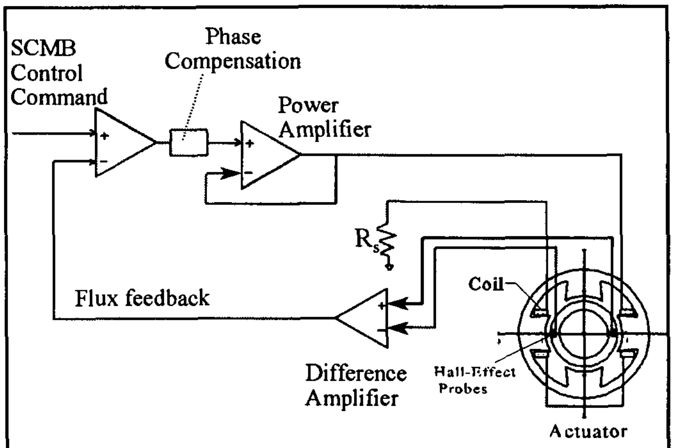

Figure 7 - Actuator Control Diagram

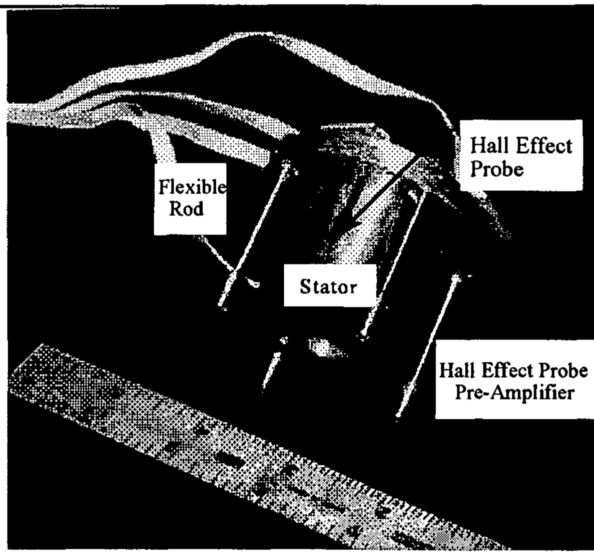

Figure 8 Stator Assembly

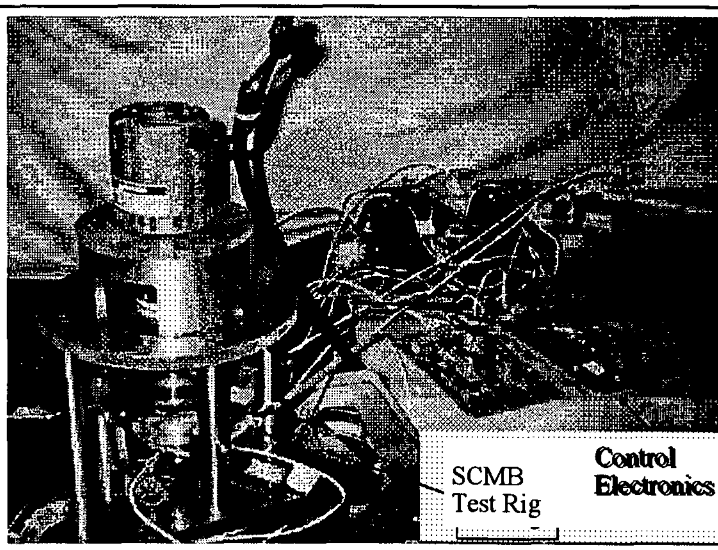

Figure 9a Experimental Setup

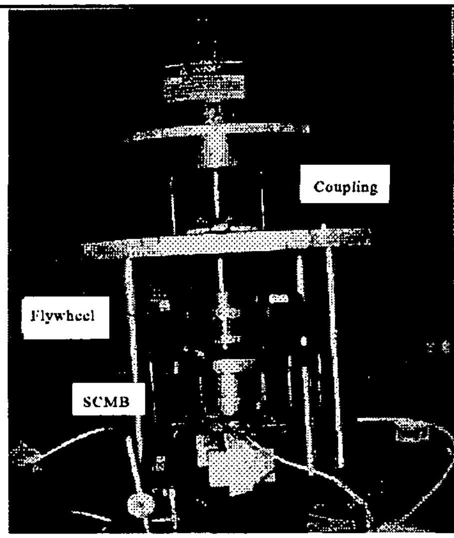

Figure 9b - A Closeup View of Test Device

TEST RESULT

Presented in Figure 9a is a picture of the test setup. There are two analog boards, one for actuator control, the other for the rotor PID control. The actuator employs two bi-polar linear power amplifiers. Figure 9b is a close view of the SCMB and the flywheel rotor. The left and middle displacement probes are used for measuring the stator motions in x and y directions. These measurements are differentiated and fed back to the actuator to achieve the stator support damping.

The flywheel rotor has been successfully levitated and rotated in the SCMB. Presented in Figure 10 are the peak-hold displacement plots recorded when coasting down from a rotor speed of 4425 rpm.

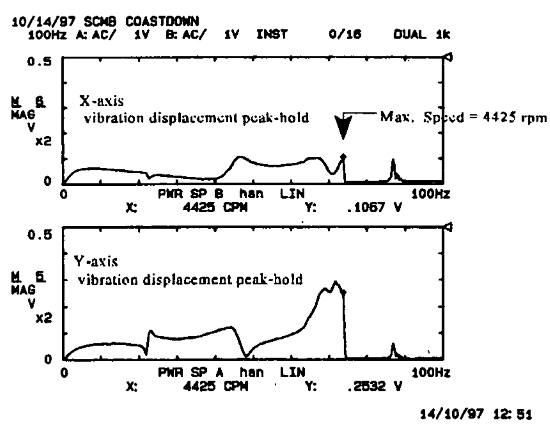

Figure 10 - SCMB Rotation Test Result

The X and Y displacement plots are quite different in amplitudes. This was a result of un-intentionally mis-tuned analog circuits which have many adjustable potentiometers. Using a digital controller would have avoided the problem and saved much tuning effort. Preventing the rotor going up to higher speeds were resonances due to the flexible column structure. The stator velocity feedback could have aggravated the resonance problem, because the probe brackets may have vibrated with the structure. Improvements of the controller and structure are being planned for operating the test rotor at higher speeds.

CONCLUSIONS

- The stator-controlled magnetic bearing has no protruding poles to face the rotor; its magnetic flux in air gaps are uniform circumferentially. There is no concern of eddy current or magnetic hysteresis losses.

- Since it is an actively controlled magnetic bearing, its stiffness and damping properties can be electronically manipulated.

- It is ideal for supporting high speed rotors, such as those of momentum and energy storage flywheels.

- A concise formulation of the rotor and stator control dynamics and a procedure for determining the system parameters to achieve stability have been presented in this paper.

- Experimental results have proved the feasibility of the new bearing concept.

ACKNOWLEDGMENT

This development work was partially sponsored by an U.S. Air Force contract F29601-97-C-0092 for which Lieutenant Jonathan Jensen of Phyllis Laboratory at Kirtland AFB, NM was the project monitor.

REFERENCES

Chen, H.M. & Walton, J., 1996. "Novel Magnetic Bearings for a Flywheel Energy Storage System" Presented at *ISROMAC-6*, Honolulu, Feb. 25-29.

Chen, H.M., 1997. "Design of a Stator-Controlled Magnetic Bearing," Proceedings of 4th International Symposium on Magnetic Suspension Technology, Gifu, Japan, Oct. 30 - Nov. 1.

Oka, K. and Higuchi, T., 1994. "Magnetic Suspension System with Permanent Magnet Motion Control," *Proceedings of the 4th International Symposium on Magnetic Bearings*, pp 317-320.

Knospe, C.R. and Stephens, L.S., 1996, " Side-Pull and Stiffness of Magnetic Bearing Radial Flux Return Paths," *ASME, Journal of Tribology*, Vol. 118, pp 98-101, January.